Nonaffine Deformation and Elasticity of Polymer Networks

Nonaffine Deformation and Elasticity of Polymer Networks

Michael Rubinstein*

Department of Chemistry, University of North Carolina, Chapel Hill, North Carolina 27599-3290

Sergei Panyukov

P. N. Lebedev Physics Institute, Russian Academy of Sciences, Moscow, Russia 117924

Received March 18, 1997; Revised Manuscript Received September 19, 1997[⊗]

ABSTRACT: We demonstrate that the origin of the nonlinear elasticity of polymer networks rests in their nonaffine deformations. We introduce the affine length R_{aff}, which separates the solid-like elastic deformations on larger scales from liquid-like nonaffine deformations on smaller scales. This affine length grows with elongation λ as $R_{aff} \sim \lambda^{3/2}$ and decreases upon compression as $R_{aff} \sim \lambda^{1/2}$. The behavior of networks on scales up to R_{aff} is that of stretched or compressed individual chains (we call them affine strands). The affine strands are stretched in the elongation direction and confined and folded in the effective tubes in the compression direction. The fluctuations of affine strands determine the diameters of the confining tubes a, which change nonaffinely with the network deformation $a \sim \lambda^{1/2}$. Our model gives a unified picture of deformations of both phantom and entangled networks and leads to a stress−strain relation that is in excellent agreement with experiments.

1. Introduction

A polymeric network is a unique state of matter because its behavior is based on the fine interplay of the solid-like and the liquid-like degrees of freedom. On macroscopic length scales it behaves as a highly deformable elastic solid. But on microscopic length scales individual chains move relatively freely as in a polymeric liquid. It is convenient to define an affine length scale R_{aff} separating the single chain behavior from the elastic many-chain one. This affine length is the shortest scale at which the parts of the network deform proportionally to the deformation of the network as a whole (deform affinely). At length scales shorter than the affine length R_{aff} the deformation is nonaffine and is characterized by the conformations of the individual network chains.

The elasticity of polymer networks is entropic in nature. It is controlled by network deformations on nonaffine length scales. The challenging problem is to develop a molecular model of these nonaffine network deformations. The most important question of rubber elasticity is how the macroscopic deformation of the network is transmitted down to the individual chains. The first model that successfully described rubber elasticity was the phantom network model,[1−3] which ignored the topological interactions between chains. In this model the deformation of the network is transmitted down to the individual chains only through their ends. In section 2 we analyze in detail the deformation of the individual chains of the phantom network. We analyze this phantom network model by separating the solid-like and liquid-like degrees of freedom. The solid-like degrees of freedom are represented by an elastic nonfluctuating solid to which the individual chains are coupled. The strength of this coupling depends on the stiffness of the local environment of the chain.[4] This coupling is modeled by effective virtual chains connecting the ends of a network chain to the elastic nonfluctuating solid. We find that a network chain elongates almost affinely if it is longer than the virtual chains connecting it to the elastic nonfluctuating solid. In the opposite case of a loose local environment (long virtual chains) a network chain is almost undeformed. Network swelling leads to the disinterpenetration of such chains.[5]

One of the most successful ways to account for the topological interactions between the network chains is the tube model.[6] In this model the network chain is confined by the neighboring ones to a tube-like region. The important question is how the diameter a of this confining tube changes with the network deformation λ. In the Edwards model[6] it was assumed that the tube diameter changes affinely with the macroscopic deformation of the network, $a \sim \lambda$. This assumption leads to some predictions that do not agree well with experiments.[7] There have been many attempts to modify the tube model in order to improve its agreement with experiments.[8−13] Unfortunately, none of them resulted in a self-consistent satisfactory picture of entangled networks.

In section 3 we propose a simple model of nonaffine confining tubes that we hope will be the first step toward such a picture. The main result of the model is that *the tube diameter changes nonaffinely*

$$a \sim \lambda^{1/2}$$

We demonstrate that this result satisfies the condition of topological invariance under the network deformation. This condition was explicitly enforced in a replica variant of this model presented in the earlier work of one of us.[14]

The attractive feature of our model is that it provides a unified physical picture of the deformation of both phantom and entangled networks. This picture is based on the separation of liquid-like and solid-like degrees of freedom. Both networks deform affinely on scales larger than the affine length R_{aff}. Deformation of both networks on length scales smaller than R_{aff} can be described by the elongation of the individual chains. The major difference between the two models is that R_{aff} in phantom networks changes affinely with the network deformation

$$R_{aff} \sim \lambda \quad \text{(phantom)}$$

while in our tube model it changes nonaffinely

$$R_{aff} \sim \begin{cases} \lambda^{3/2} & \text{for } \lambda > 1 \\ \lambda^{1/2} & \text{for } \lambda < 1 \end{cases} \quad \text{(nonaffine tube model)}$$

In section 4 we calculate a stress−strain relation for deformed networks based on our simple model. We demonstrate excellent agreement between our predictions and experiments on radiation-cured polybutadiene networks.

2. Phantom Network

We begin our study of deformations in polymeric networks from the simplest model—the phantom Gaussian network. Consider a concentrated polymer solution or melt of Gaussian chains.[15] Let us assume that we have instantaneously formed a network from an equilibrium solution or melt. This can be achieved either by the instantaneous cross−linking or by the end−linking of chains. After formation of the network, the chains "realize" that they are no longer free to move through the system but are constrained by the cross−links. From now on we will define a chain as a linear section between two cross−links, even though it could have been a part of a multiply cross−linked original chain. We do not consider dangling ends of the network, because they can completely relax even in the stretched network and do not contribute to its elasticity.

Let us consider the conformations of a test chain of N monomers. The only way the chain "knows" that it is a part of a phantom network is because its ends (cross−links) are no longer free but are localized and can only fluctuate around some average positions. There are two factors that define the amplitude of such fluctuations: the elasticity of the test chain and the elastic properties of the network at those places where the chain is connected to it (Figure 1a). Therefore it is convenient to consider the fluctuations of the network without the test chain. The local stiffness of such network at the two potential cross−link points can be described by the mean square amplitude ξ_i^2 of fluctuations of these potential cross−links, $i = 1, 2$, around their average positions $\mathbf{X}_i$. One can represent the fluctuations of a potential cross−link by the fluctuations of the free end of an n_i-mer ("virtual chain"), the other end of which is attached at position $\mathbf{X}_i$ inside an elastic nonfluctuating solid (see Figure 1b). These attachment points displace affinely with the deformation of the network. The number of monomers n_1 and n_2 of such virtual chains represents the fluctuations ξ_1 and ξ_2 of the network at the places where the test chain is connected to it, $n_i = (\xi_i/b)^{1/2}$ for $i = 1, 2$, where b is the monomer size (persistence length).

The monomers of virtual chains undergo thermodynamic fluctuations like the native chains of the network. Since the fluctuations of the cross−links are independent,[16] the mean square fluctuations of the vector between these potential cross−links without the test chain attached to them is $\xi^2 = \xi_1^2 + \xi_2^2 = b^2 n$, where $n = n_1 + n_2$ is the total number of monomers comprising the two virtual chains. The value ξ^2 defines the elastic free energy, $\approx kT\mathbf{R}^2/\xi^2$, of deformations having a distance $|\mathbf{R}|$ between the two potential cross−links, and thus, the effective elastic modulus between these points is kT/ξ^2 (k is the Boltzmann coefficient, and T is the temperature).

The local stiffness of the network varies from one region to another because of the irregularities of the
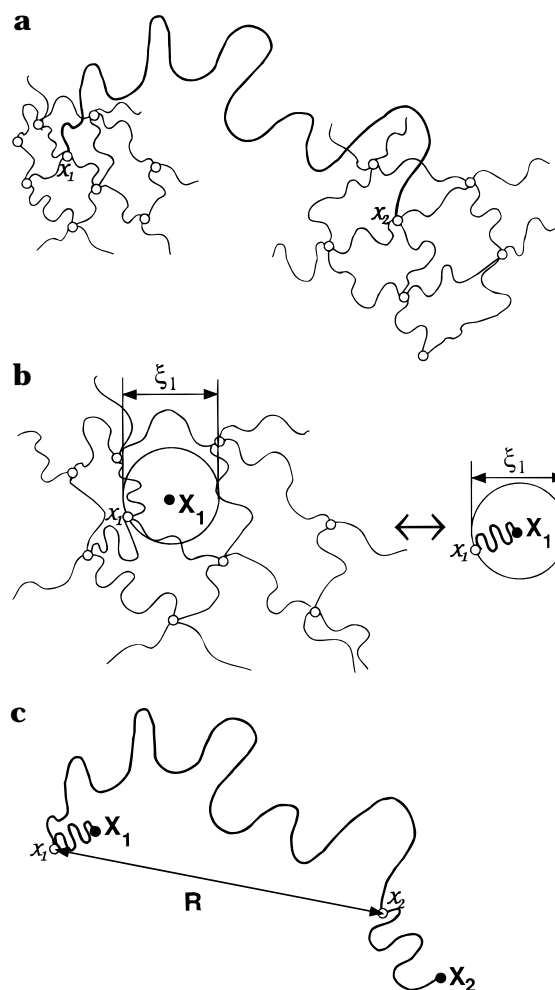
Figure 1. Combined chain of a phantom network. (a) A strand is connected to the network by its ends. The chains of the network, sketched by thin lines, are determining the local elastic environment at the ends of the strand. (b) The fluctuations of the potential cross-link $\mathbf{x}_1$ around its average position $\mathbf{X}_1$ by a typical distance ξ_1 can be represented by a virtual chain. The number of monomers of the virtual chain is $n_1 = (\xi_1/b)^2$. (c) The combined chain consists of the network strand of N monomers and two virtual chains of n_1 and n_2 monomers. The virtual chains connect the network strand to the nonfluctuating elastic solid at points $\mathbf{X}_1$ and $\mathbf{X}_2$.

network structure. These variations lead to corresponding variations of the values of ξ_1 and ξ_2 (or ξ) about their average values. In the case of networks prepared by cross−linking of linear chains, one can estimate the average elastic modulus between any two potential cross-links to be $kT/(b^2\bar{N})$, where $\bar{N}$ is the average number of monomers of the network chains. This estimate gives us the value of the mean-squared fluctuations of the distance between the potential cross−links $\overline{\xi^2} \simeq b^2\bar{N}$ averaged over the volume of the network. Here the bar is used to distinguish averaging over the volume of the network from thermodynamic averaging. The distribution function of the fluctuation length ξ is peaked near its average value $(\overline{\xi^2})^{1/2}$. The width of the peak grows with increasing polydispersity of the chain lengths. A method of calculating this distribution function for a given network structure was proposed by Ball and Higgs[4] on the basis of the analogy with the calculations of the conductivity of the resistor network. We shall not discuss these calculations in the present paper.

The key to finding the distribution function of the average positions $\mathbf{X}_l$ of the potential cross−links without the test chain (points of attachment of the virtual chains to the elastic solid) is to consider the equilibrium process of the network formation. We can consider three independent stages in the network preparation: (i) and (ii) preparation of the two regions of the elastic medium with one available potential cross−link in each with the vector $\mathbf{R}$ between the two potential cross−links; (iii) choosing a free polymer chain of N monomers with an end-to-end vector $\mathbf{R} = \mathbf{x}_1 - \mathbf{x}_2$, which can be connected to these potential cross−links. The probabilities of the first two events, $P_{n_1}(\mathbf{X}_1 - \mathbf{x}_1)$ and $P_{n_2}(\mathbf{x}_2 - \mathbf{X}_2)$, are defined by the elastic free energy of two virtual chains of total length $n = n_1 + n_2$, discussed above. The probability of the last event is $P_N(\mathbf{x}_1 - \mathbf{x}_2)$. Here $P_N(\mathbf{x})$ is the end-to-end correlation function of the Gaussian chain

$$P_N(\mathbf{x}) = (2\pi b^2 N)^{-3/2} \exp\left(-\frac{\mathbf{x}^2}{2b^2 N}\right) \qquad (1)$$

The probability of finding the vector $\mathbf{X}_{12} \equiv \mathbf{X}_1 - \mathbf{X}_2$ is the product of the probabilities of all three independent stages. To find the distribution function of the vector $\mathbf{X}_{12}$, we have to sum over all allowed positions $\mathbf{x}_1$ and $\mathbf{x}_2$ of potential cross−links

$$\int d\mathbf{x}_1 \, d\mathbf{x}_2 \, P_{n_1}(\mathbf{X}_1 - \mathbf{x}_1) \, P_N(\mathbf{x}_1 - \mathbf{x}_2) \, P_{n_2}(\mathbf{x}_2 - \mathbf{X}_2) = $$
$$P_{N+n_1+n_2}(\mathbf{X}_1 - \mathbf{X}_2)$$

This distribution function is Gaussian and coincides with that of an effective "combined" chain of $n + N$ monomers. The "combined" chain is connected by its ends to the nonfluctuating elastic medium, which deforms affinely with the sample (see Figure 1c). The components of the end-to-end vector of the combined chain also deform affinely upon deformation of the network by factors λ_α along the corresponding principal directions $\alpha = x, y, z$

$$[\mathbf{X}_{12}(\lambda_\alpha)]_\alpha = \lambda_\alpha [\mathbf{X}_{12}(\lambda_\alpha = 1)]_\alpha \qquad (2)$$

We shall omit below the argument $\lambda = 1$ in the case of the undeformed network, $\mathbf{X}_{12}(\lambda=1) \equiv \mathbf{X}_{12} = \mathbf{X}_1 - \mathbf{X}_2$

The network strand of N monomers can be thought of as a section of the combined chain. Consider the dependence of the mean square size $\langle \mathbf{R}^2 \rangle = \langle (\mathbf{x}_1 - \mathbf{x}_2)^2 \rangle$ of this strand on the local elasticity of the network, ξ, and the deformation ratios, λ_α. Note that we can restrict our attention to only one principal direction α of network deformation because of the independence of fluctuations of a Gaussian network in different directions.

The mean square size of this strand can be expressed as

$$\langle R^2 \rangle = \langle R \rangle^2 + \langle (\Delta R)^2 \rangle \qquad (3)$$

in terms of the average end-to-end distance of the strand, $\langle R \rangle$, and its mean square fluctuation, $\langle (\Delta R)^2 \rangle = \langle (R - \langle R \rangle)^2 \rangle$. To find $\langle R \rangle$ we consider the combined chain of $n+N$ monomers deformed by the factor λ with the average end-to-end distance $b(n + N)^{1/2}\lambda$. The strand deforms linearly with the deformation of the combined chain

$$\langle R \rangle = \frac{N}{n + N} b(n + N)^{1/2}\lambda = \frac{\lambda b N}{(n + N)^{1/2}} \qquad (4)$$

The fluctuations of the end-to-end distance of the network strand are dominated by the shorter of the two chains: (i) the strand and (ii) the sum of the two virtual chains. The mean square fluctuations of the end-to-end vector of the network strand can be calculated by assuming a parallel connection of the strand of N monomers and the virtual chain of n monomers:

$$\langle (\Delta R)^2 \rangle = \frac{b^2}{1/N + 1/n} \qquad (5)$$

If the network is locally stiff, the virtual chains are short and the fluctuations of the end-to-end vector of the network strand are suppressed ($\langle (\Delta R)^2 \rangle \simeq b^2 n$ for $N > n$). But if the network is locally soft, the fluctuations of the end-to-end vector of the short strand ($N < n$) are limited by its size, $\langle (\Delta R)^2 \rangle \simeq b^2 N$. Substituting eqs 4 and 5 into (3) we finally find the mean square size of the network strand

$$\langle R^2 \rangle = \frac{\lambda^2 b^2 N^2}{n + N} + \frac{b^2}{1/N + 1/n} = b^2 N \frac{n + \lambda^2 N}{n + N} \qquad (6)$$

Our main conclusion is that both the elastic properties of the strand itself (e.g., its length N) and the local elastic environment of the network at both ends of the strand determine how it deforms. The local elasticity of the network is controlled by the fluctuations of the positions of the potential cross−links. If these fluctuations are small compared to the chain size (stiff local environment), the strand deforms almost affinely. If they are large (loose local environment) the strand deforms only slightly. Similar results were obtained in a different form by Higgs and Ball.[4]

3. Entangled Networks

3.1. Nonaffine Tube Model. We now proceed to consider the elasticity of the entangled network. The main difference between phantom and entangled networks is that in the former the stress of the network is transmitted to the chain only through its ends, whereas in the latter it is also transmitted through the topological constraints along the whole length of the chain. The topological constraints imposed on a given chain by its neighbors confine it to a tube-like region,[6] see Figure 2a. This confining tube restricting the fluctuations of the chain can be represented by an effective "topological potential" acting on the monomers of the chain. The simplest form of this confining potential is the harmonic potential, proposed by Edwards[6] about 30 years ago. In light of the simple model outlined in the previous section, the harmonic confining tube potential is equivalent to a set of harmonic virtual chains acting on the test chain. One can divide the test chain of N_{tot} monomers into N_{tot}/N fragments of N monomers each and attach the junction points of such fragments to the virtual chains. The other ends of these virtual chains are connected to the nonfluctuating elastic solid. The picture of such a comb polymer is shown in Figure 2b. The number n of monomers in the virtual chains is related to their mean square fluctuation $\xi^2 = b^2 n$ in the absence of the test chain. For simplicity we neglect the distribution of the elastic moduli kT/ξ^2 between different virtual chains corresponding to different regions of the network (this effect in phantom networks was discussed in detail in the previous section). We also neglect large scale chain diffusion along the effective tube, which is
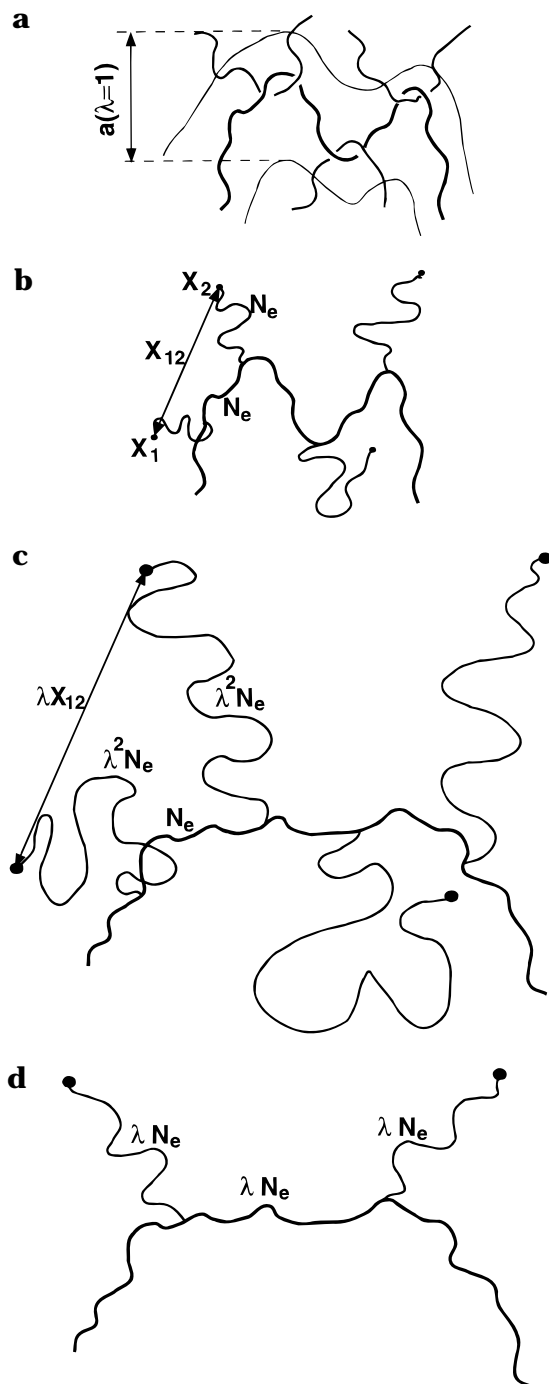
a

b

c

d

Figure 2. Test chain of an entangled network. (a) The test chain is confined by the neighboring chains to a tube-like region. (b) The confining potential of the tube can be represented by the virtual chains. There are N_e monomers of the test chain between neighboring junction points with the virtual chains. Virtual chains are connecting the test chain to the nonfluctuating elastic solid at points $\mathbf{X}_i$. In the preparation state virtual chains have N_e monomers. (c) The conformation of the test chain in the swollen network shows that the virtual chains contain $\lambda^2 N_e$ monomers. Points of attachments of the virtual chains to the nonfluctuating elastic solid deform affinely. (d) λ neighboring virtual chains of the swollen network can be replaced by a single stiff one containing λN_e monomers.

prohibited in the presence of permanent cross−links of the test chain with the network.

It is shown in the Appendix that the mean square fluctuations of the test chain monomers (the tube diameter) with $N \lesssim n$ are $a^2 = b^2(Nn)^{1/2}$. We can therefore choose any pair of parameters N and n (the condition that the fluctuations of middle points between

junctions should not differ from the junction fluctuations imposes the constraint $N < n$[17]) such that

$$nN = \text{const} \qquad \text{for} \quad N < n \qquad (7)$$

The key to understanding such "gauge" invariance lies in the fact that a group of $l = N'/N$ consecutive virtual chains connected to the test chain can be replaced by one effective virtual chain with elastic modulus $kT/(b^2 n')$ $= lkT/(b^2 n)$ (parallel connection of l springs). Thus we get shorter (stiffer) virtual chains, $n' = n/l$, separated by longer strands of the test chain, $N' = Nl$, but the product of the degrees of polymerization $N'n' = Nn$ is left invariant.

The degree of polymerization between entanglements at the network preparation conditions is denoted by N_e and the tube diameter by $a = bN_e^{1/2}$ (the mean square fluctuation of monomers $a^2 = b^2 N_e$). We could attach a virtual chain to every strand of N_e monomers (one virtual chain corresponds to one entanglement—see Figure 2b). Alternatively, we could place weaker virtual chains $n > N_e$ with fewer monomers $N = N_e^2/n$ between attachment points. In both cases the mean square fluctuation of the monomers of the test chain will be $\sim a^2 = b^2 N_e$.

In close analogy with the results of the previous section, the two-point distribution function of the positions $\mathbf{X}_i$ and $\mathbf{X}_j$ ($i < j$) of the points of attachment of virtual chains to the elastic solid is described by the combined chain model consisting of the test chain of $(j - i)N$ monomers and two virtual strings of n virtual monomers each. Using the results of this model, we find the mean square vector $\mathbf{X}_{ij} \equiv \mathbf{X}_j - \mathbf{X}_i$ between these points

$$\overline{(\mathbf{X}_{ij})^2} = b^2[|j - i|N + 2n] \qquad (8)$$

Note that there are $j - i - 1$ virtual side chains connecting the strand of $(j - i)N$ monomers to the elastic solid in addition to two virtual chains at the end of the strand. These virtual side chains do not affect the quenched mean square vector (eq 8) because we average over the coordinates of the points of their attachments to the elastic solid.

The positions of the attachment points deform affinely with the network deformation, as in the phantom network model (section 2):

$$[\mathbf{X}_{ij}(\lambda_\alpha)]_\alpha = \lambda_\alpha[\mathbf{X}_{ij}(\lambda_\alpha=1)]_\alpha \qquad (9)$$

Here λ_α are the deformation ratios of the network along the corresponding principal directions $\alpha = x, y, z$.

The major feature of the present model of entangled networks, which distinguishes it from others models, is *the dependence of the strength of the confining potential* (elasticity of virtual chains) *on the network deformation*. Recall that in the previous section we assumed that the elastic constants of virtual chains did not change with the deformation of phantom networks. This is a valid assumption for Gaussian phantom networks.[18] A similar assumption was made by Edwards for entangled networks.[6] It was implicitly assumed in his model that the strength of the confining potential does not change with the network deformation. But the confining potential due to the topological interactions determines how far a given chain can fluctuate before it is constrained by its neighbors. It is therefore very natural to assume that these fluctuations (the diameter of the confining tube) change upon

network deformations, as chains move closer together or further apart. The average distance between chains changes affinely with the network deformation. Thus, we assume that the fluctuations of virtual chains that characterize the topological stiffness of local enviroment deform affinely with the network.

$$\xi_\alpha(\lambda_\alpha) = \lambda_\alpha \xi(\lambda_\alpha = 1) \qquad (10)$$

Equation 10 is the main assumption of our model, which is valid both for isotropic and for anisotropic deformations. In the latter case the local topological environment becomes anisotropic. It depends on the effective harmonic topological potential (virtual chains) that splits into three independent harmonic potentials in the principal directions of the deformation.

For nonphantom Gaussian networks this leads to the splitting of the three−dimensional problem into three one−dimensional ones. Therefore it is enough to consider the case of the deformation by a factor λ in a particular principal direction. The simplest case of isotropic swelling in which all the directions are equivalent is considered in the following section.

In the case of isotropic deformations (swelling), $\lambda_x = \lambda_y = \lambda_z = \lambda$, the fluctuations of the virtual chains remain isotropic $\xi_x(\lambda) = \xi_y(\lambda) = \xi_z(\lambda) = \lambda\xi(1)$. In the case of anisotropic deformations (e.g., $\lambda_y = \lambda_z = 1/\sqrt{\lambda_x}$), the fluctuations of virtual chains become anisotropic, leading to anisotropically deformed tubes (see section 4 below).

3.2. Deformed Network. For simplicity, we begin with the description of the case of isotropic swelling. The same description can be applied to the principal direction of elongation in anisotropically deformed networks (e.g., along the elongation axis for uniaxial elongation). If the network is swollen by a factor λ, the fluctuations of virtual chains change affinely $\xi(\lambda) = bn^{1/2}(\lambda) = \lambda\xi(1) = \lambda b[n(1)]^{1/2}$. Therefore the number of "monomers" in the virtual chains of the deformed network is $n(\lambda) = n(1)\lambda^2$ and the mean square fluctuation of the test chain (deformed tube diameter) is

$$a^2(\lambda) = b^2[Nn(\lambda)]^{1/2} = b^2[Nn(1)]^{1/2}\lambda = a^2(1)\lambda$$

The above equation shows that the tube diameter deforms nonaffinely

$$a(\lambda) = a(1)\lambda^{1/2} \qquad (11)$$

It is important to note the different physical meaning of the tube diameter $a(\lambda)$ (eq 11) and the fluctuations of virtual chains $\xi(\lambda)$ (eq 10). The latter ($\xi(\lambda)$) characterizes the topological stiffness of the local environment, while the former ($a(\lambda)$) is the mean fluctuation of the monomers of the chains, which is determined by both the local topological environment and the stiffness of the chain itself.

The test chain is attached to several virtual chains of $n\lambda^2$ virtual monomers each. The section of the test chain between neighboring junction points has N monomers (Figure 2c). Since $n\lambda^2 > N$, each virtual chain is softer than the strand of the test chain between junction points and does not significantly deform the test chain. But we can replace $l = N_e\lambda/N$ virtual chains by a single one without any significant effect on the configurations of the test chain; see Figure 2d. This replacement leads to the same number of monomers in a virtual chain and a strand of the test chain between junction points, $N' = n' = N_e\lambda$. In this case each virtual chain makes a

significant contribution to the configuration of the test chain (modifies its trajectory). The fluctuations of these virtual chains and of the strands of the test chain between junction points are of the order of the deformed tube diameter, $a(\lambda) = b(N_e\lambda)^{1/2} = a(1)\lambda^{1/2}$; see eq 11. If we consider the undeformed test chain with the same number of monomers, λN_e, between junction points, the number of monomers in the virtual chain would be N_e/λ. The mean square distance between the points of attachment of the nearest virtual chains to the affine solid is (see eq 8 for $j = i + 1$)

$$\overline{(\mathbf{X}_{i+1} - \mathbf{X}_i)^2} \simeq b^2 N_e/\lambda + 2b^2 N_e\lambda$$

For the elongation ($\lambda > 1$) it is determined by the length of the test chain strand, while for the compression ($\lambda < 1$), it is determined by the length of the virtual chains. After the affine deformation this distance becomes

$$\lambda[\overline{(\mathbf{X}_{i+1} - \mathbf{X}_i)^2}]^{1/2} \simeq \begin{cases} bN_e^{1/2}\lambda^{3/2} & \text{for} \quad \lambda \gg 1 \\ bN_e^{1/2}\lambda^{1/2} & \text{for} \quad \lambda \ll 1 \end{cases}$$

The distance between the points of attachment of the neighboring virtual chains is of the order of the length of the strand between the junction points of the deformed test chain (since $N' = n'$). Note, that in the case of elongation ($\lambda > 1$) the stretched size of this strand of $N' = N_e\lambda$ monomers is λ times longer than the undeformed size of the same strand, $b(N_e\lambda)^{1/2}$, implying that it deforms affinely. Therefore, the size of this strand of $N_e\lambda$ monomers is the affine length scale in the stretched networks

$$R_{\text{aff}} = bN_e^{1/2}\lambda^{3/2} \qquad \text{(elongation)} \qquad (12)$$

The test chain is stretched by the virtual chains up to this length scale. At larger length scales the virtual chains affinely deform the test chain. The reason for this affine deformation is in the correlation of the points of attachments of the virtual chains to the affine nonfluctuating solid along the confining tube of the test chain.

It is important to emphasize that since the test chain is stretched on length scales shorter than the affine length, the size of the stretched subchain of N_e monomers is $N_e/(N_e\lambda) = 1/\lambda$ of the affine length. Therefore it is just equal to the deformed tube diameter, $bN_e^{1/2}\lambda^{1/2}$. This proves that our choice for the rescaling of the virtual chains' size with the network deformation was the correct one. Indeed, it leads to a tube diameter (fluctuation length scale of an affine strand) equal to the deformed size of the entanglement strand of N_e monomers.

3.3. Compression. Below we describe the isotropic deswelling of entangled networks. The same description can be applied to the principal direction of compression in the anisotropically deformed networks. The deformed tube diameter of the compressed network ($\lambda < 1$), $bN_e^{1/2}\lambda^{1/2}$, is smaller then that of the undeformed one ($bN_e^{1/2}$), and the strand of the size between neighboring virtual chains contains fewer monomers than the original entanglement strand ($N_e\lambda < N_e$). We note that these virtual chains in the undeformed configuration contain N_e/λ monomers and connect the test chain to the regions of the network outside the original tube ($bN_e^{1/2}/\lambda^{1/2} > bN_e^{1/2}$). These topological interactions (modeled by the virtual chains), though weak ($<kT$ of stored energy) in the undeformed network, become important in the

contracted state. The initially remote sections of the network near the points of attachments of virtual chains to the affine solid get folded into the test chain and introduce "additional" topological constraints, making the effective degree of polymerization between entanglements shorter. We put "additional" in quotes because these topological interactions were already present in the undeformed network (the topology is fixed at the moment of cross—linking and does not change upon deformation). The weakness of the virtual chains related to these topological interactions in the undeformed network implies that each of them separately does not affect confinement of the test chain in any major way. But collectively these weak virtual chains confine an undeformed test chain into its tube. These individually weak, but numerous, virtual chains became important only upon contraction, confining the test chain into a much tighter entanglement net (narrower tube).

Another important feature of the network contraction arises from the fact that the mean square distance between points of attachment of the virtual chains to the affine solid in the undeformed network is $(\mathbf{X}_{l+1} - \mathbf{X}_l)^2 \simeq b^2 N_e / \lambda$ for all $l < 1/\lambda^2$ (that is until the separation of the junction points between the test chain and the virtual chains becomes of the order of the size of virtual chains, $l N_e \lambda \simeq N_e / \lambda$); see eq 8. This implies that upon contraction all these $l = 1/\lambda^2$ consecutive attachment points get squeezed into one tube diameter $\lambda[(\mathbf{X}_{k+l} - \mathbf{X}_k)^2]^{1/2} = b N_e^{1/2} \lambda^{1/2} \simeq a(\lambda)$. Therefore $1/\lambda^2$ consecutive strands of $N_e \lambda$ monomers get folded into the same length scale of $a(\lambda)$. Thus, the size of the strand of the test chain of N_e / λ monomers is almost the same as the size of the strand of $N_e \lambda$ monomers and this length defines the affine length of the compressed network

$$R_{aff} \approx a(\lambda) = b N_e^{1/2} \lambda^{1/2} \quad \text{(compression)} \quad (13)$$

The points of attachment of virtual chains to the affine solid that are separated by more then N_e / λ monomers of the test chain do not contract into the same region of the network.

The long virtual chains in the undeformed state imply the existence of topological interactions in the network extending well beyond the diameter of the tube. The physical origin of these extended topological interactions is the following: In the contracted state the test chain is confined to a narrow tube. This means that the strands of the network are overlapping with it, imposing "additional" topological constraints and making the degree of polymerization between such additional entanglements shorter. But the topology of the network was fixed in the preparation state. Therefore, the same "additional" topological constraints exist both in contracted and in undeformed states. They are imposed by the chains that are outside the tube of the test chain in the undeformed state, but overlap with it in the contracted state. The effect of these topological constraints on the confinement of the test chain is much stronger in the contracted state than in the undeformed one.

3.4. Short Summary. We can summarize our understanding of the behavior of the chain on different scales by the following simple equation for the mean square distance between monomers i and j of the chain separated by $N = |i - j|$ monomers:

$$\langle R_N{}^2 \rangle \approx b^2 N \frac{N_e \lambda + \lambda^2 N}{N_e \lambda + N} \quad (14)$$

Notice that this expression is analogous to eq 6 for the mean square size of the chain of N monomers in the phantom network with the number $n = N_e \lambda$ of monomers of the virtual chain. But we stress that eq 14 has a different meaning since it describes the deformations of a chain confined in a typical tube rather than a phantom chain connected to the network by its ends. This analogy is not surprising because of the same underlying physics that was laid in the foundation of both models. Equation 14 clearly shows that the chains of the entangled network deform affinely only on scales larger than the affine length R_{aff} defined by eqs 12 and 13.

4. Stress in Deformed Polymer Networks

In the phantom Gaussian networks the distance between the end points of a typical strand of $\overline{N}$ monomers varies affinely with the network deformation. The stretched strand stores $kT\lambda^2$ of elastic energy. The number density of strands is $c/\overline{N}$, where c is the monomer concentration. This leads to the well-known estimate for the free energy density of a phantom network $kT\lambda^2(c/\overline{N})$. The free energy density of anisotropically deformed Gaussian networks can be found from the fact that the fluctuations of monomers are independent in different principal directions of deformations:

$$F_{ph}(\lambda) \simeq kT \frac{c}{\overline{N}} \sum_\alpha \frac{\lambda_\alpha{}^2}{2} = G_c \sum_\alpha \frac{\lambda_\alpha{}^2}{2} \quad (15)$$

where λ_α is the network expansion factor in the α-direction and G_c is the shear modulus of the phantom network $G_c = kTc/\overline{N}$.[19]

We can apply the above ideas to find the free energy of entangled networks. Consider the case of a network isotropically swollen by a factor $\lambda > 1$. The main difference between entangled and phantom networks is that in the former the number of monomers in the affine strand, $N_e \lambda$, depends on network deformation λ. Each such strand deforms affinely with the network deformation and carries $kT\lambda^2$ of elastic energy. Thus the free energy density of a stretched entangled network can be estimated as $kT\lambda^2[c/(N_e\lambda)] = kTc\lambda/N_e$. In the case of isotropic compression, $\lambda < 1$, the strand of $N_e\lambda$ monomers is not stretched but rather forms a loop that stores kT of free energy. Therefore the free energy density of a compressed entangled network is equal to $kTc/(N_e\lambda)$. Using the above estimates, we can construct the following simple expression for an isotropically deformed entangled network $F_{ent} \simeq kT(c/N_e)(\lambda + 1/\lambda)$, which smoothly crosses between the stretched ($\lambda > 1$) and compressed ($\lambda < 1$) cases.

The mean-squared monomer fluctuations $\xi_\alpha(\lambda_\alpha) = b(N_e\lambda_\alpha)^{1/2}$ of an anisotropically deformed network depend on the principal directions of the network deformation $\alpha = x, y, z$. The free energy density of a Gaussian nonphantom network is the sum of the contributions from these principal directions

$$F_{ent}(\lambda) \simeq kT \frac{c}{N_e} \sum_\alpha \left(\lambda_\alpha + \frac{1}{\lambda_\alpha} \right) = G_e \sum_\alpha \left(\lambda_\alpha + \frac{1}{\lambda_\alpha} \right) \quad (16)$$

where $G_e = kTc/N_e$. Note that G_e is equal to the plateau modulus of entangled polymer solutions or melts before cross-linking.[20] Using eqs 15 and 16, we finally find the expression for the elastic free energy density of an anisotropically deformed network

$$F(\lambda) \simeq F_{ph}(\lambda) + F_{ent}(\lambda) \qquad (17)$$

which interpolates between the cases of phantom and entangled regimes of deformation. A qualitatively similar expression for the free energy $F(\lambda) \simeq \sum_\alpha (E_1\lambda_\alpha + E_2\lambda_\alpha^2)$ was proposed[21] to describe the experimental data on uniaxial and biaxial stretching. The analogous expression was proposed a long time ago[22] for the free energy of compressed gels $F(\lambda) \simeq \sum_\alpha (C''/\lambda_\alpha + C'\lambda_\alpha^2)$.

We now apply the above free energy density (eq 17) to find the stress−strain dependences for a uniaxially deformed incompressible network with $\lambda_x = \lambda$ and $\lambda_y = \lambda_z = 1/\sqrt{\lambda}$. For $\lambda > 1$ the network is stretched in the x-direction and compressed in the y- and z-directions. The typical chain of the network is elongated along the x-axis on the affine scale $bN_e^{1/2}\lambda^{3/2}$ and is confined in the y- and z-directions on the scale of the tube diameter $a(1/\sqrt{\lambda}) = bN_e^{1/2}/\lambda^{1/4}$. Thus, the tube in the uniaxially deformed network becomes highly anisotropic. The force per unit area of undeformed sample needed to stretch such network by the factor λ is

$$f = \partial F(\lambda)/\partial\lambda \approx G_c(\lambda - \lambda^{-2}) + G_e(1 - \lambda^{-3/2})(1 + \lambda^{-1/2}) \qquad (18)$$

The experimental data are usually presented in the Mooney−Rivlin form

$$f^*(\lambda^{-1}) = \frac{f}{\lambda - \lambda^{-2}} = G_c + \frac{G_e}{(\lambda - \lambda^{1/2} + 1)} \qquad (19)$$

Examples of the Mooney−Rivlin plots for polybutadiene networks are presented in Figure 3a,b. The symbols in Figure 3a correspond to the networks formed by radiation cross-linking of polybutadiene melts with molecular weight 344 000 and deformed in undiluted state.[24] The lines in Figure 3a are the best fits of the data[24] to our expression $f^*(\lambda^{-1})$ (eq 19). The parameters of the fits are $G_e \simeq 0.8$ MPa for all three sets of data and $G_c \simeq 0.51$ MPa, $G_c \simeq 0.42$ MPa and $G_c \simeq 0.35$ MPa for denser, intermediately and looser cross-linked networks respectively. The value of entangled modulus G_e is very close to the measured plateau modulus of the polybutadiene melt $G_N^0 \simeq 1.16$ MPa.[24] The three fitted values of G_c are approximately proportional to the radiation doses, which should themselves be proportional to the densities of cross-links. This is consistent with our model relating the modulus G_c to chemical cross-links (eq 15).

Figure 3b represents the data for the polybutadiene networks cured in 50% tetradecane solutions with a molecular weight of 168 000. The best fits of the data to our model (eq 19) were obtained with parameters $G_e \simeq 0.17$ MPa for all three sets of data and $G_c \simeq 0.22$ MPa, $G_c \simeq 0.17$ MPa, and $G_c \simeq 0.14$ MPa. It is striking that the dependence of the modulus G_e on concentration coincides with that of the plateau modulus in polymer solutions,[25] $G_e \sim c^{2.3}$. The values of the modulus G_c are again proportional to the radiation doses, as in the dry networks.

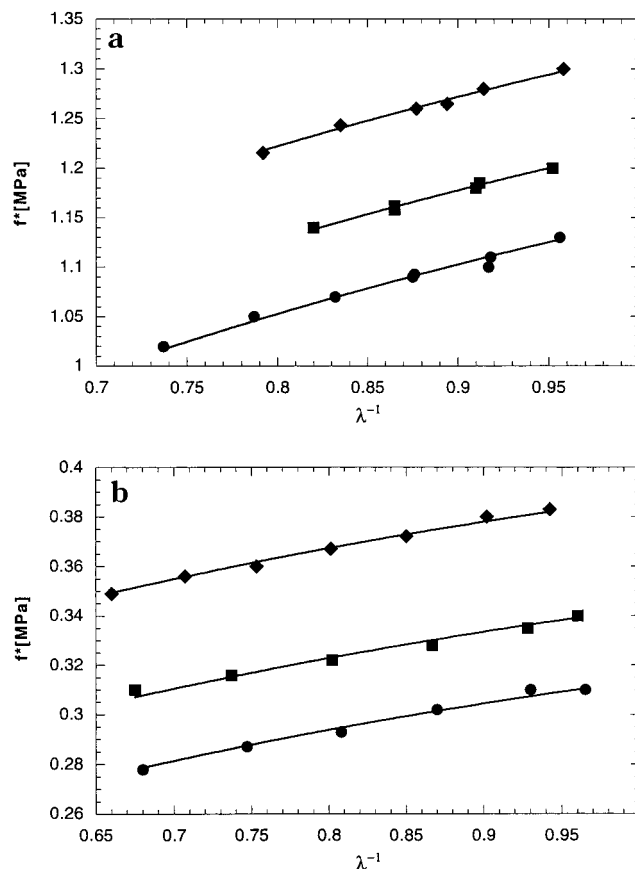The Mooney−Rivlin plot is usually fitted by the phenomenological equation

Figure 3. Mooney−Rivlin plots of the polybutadiene networks:[24] (a) networks formed by radiation cross-linking of polybutadiene melts and deformed in the undiluted state. (b) networks formed in a 50% solution of polybutadiene in tetradecane and deformed at the same concentration. Lines are the best fits to our stress−strain relation (19); see text for more details.

$$f^*(\lambda^{-1}) = 2C_1 + 2C_2\lambda^{-1} \qquad (20)$$

In the range covered by the data our fits are practically indistinguishable from the standard ones (eq 20). It is interesting to calculate the parameters of the Mooney−Rivlin equation $2C_1$ and $2C_2$ from our microscopic model. Expanding our eq 19 about the undeformed network state ($\lambda = 1$), we obtain the simple relations

$$2C_1 = G_c + \frac{1}{2}G_e$$

$$2C_2 = \frac{1}{2}G_e \qquad (21)$$

These relations were noticed for cross-linked ethylene−propylene copolymers[26] and for polybutadiene[24] and end-linked poly(dimethylsiloxane) networks. Equations 21 imply that the Mooney−Rivlin parameter $2C_2$ accounts only for half of the topological contribution to the network modulus. The parameter $2C_1$ includes the entire chemical contribution and the second half of the topological contribution. We stress that the standard interpretation of the Mooney−Rivlin parameters is quite different.[27] It is routinely assumed that the parameter $2C_1$ is only due to chemical cross-links, while the parameter $2C_2$ includes all of the topological contribution.

5. Discussion

We have proposed a unified model of both entangled and unentangled networks. We have introduced the

affine length R_{aff} that separates the two qualitatively different types of deformation. Parts of the network of sizes larger then R_{aff} deform affinely with the whole sample. The deformation picture on scales smaller then R_{aff} is that of individual stretched or compressed chains. In phantom networks the scale R_{aff} is the distance between cross-links, which changes affinely

$$R_{aff} = b\overline{N}^{1/2}\lambda \qquad \text{(phantom)}$$

Upon elongation of entangled networks, R_{aff} grows faster then the tube diameter

$$R_{aff} = bN_e^{1/2}\lambda^{3/2} \qquad \text{(elongation)}$$

and corresponds to the size of the stretched strand of $N_e\lambda > N_e$ monomers (see Figure 2d). The environment of the strand becomes looser since the surrounding chains move apart from each other. Such disinterpenetration of chains upon the network swelling has been observed experimentally.[5] The amplitude of fluctuations of monomers belonging to such strands defines the tube diameter, which grows nonaffinely:

$$a = bN_e^{1/2}\lambda^{1/2} \qquad (22)$$

A similar expression for the tube diameter was proposed several years ago to obtain the best fit of the scattering profiles of labeled chains in uniaxially deformed networks.[28-31]

The tube diameter predicted by our model (eq 22) is equal to the size of the stretched entanglement strand of N_e monomers. This result confirms the internal self-consistency of our model: the tube diameter of the deformed network is controlled by the same number of monomers between entanglements as in the undeformed one. Thus the network topology (which is characterized in our model by the number N_e of monomers between entanglements) does not change upon deformation.

Upon compression of the network the affine size decreases nonaffinely:

$$R_{aff} = bN_e^{1/2}\lambda^{1/2} \qquad \text{(compression)}$$

The number of monomers in this affine strand is N_e/λ. The conformation of this confined strand corresponds to $1/\lambda^2$ sections of $N_e\lambda$ monomers in each folded into the same volume. Therefore the tube diameter coincides with the affine length and is determined by the same expression (eq 22) as for elongation. The smallest chain strand of this size contains $N_e\lambda$ monomers and is shorter than the strand of N_e monomers between "true" entanglements. Therefore the compression reveals "additional" topological entanglements, which were already present but not important in the undeformed network. The appearance of such "additional" entanglements is due to the large number of additional strands that fold in and overlap with a given one.

Note that the simplest model of harmonic topological potential[6] utilized in the present paper does not allow the redistribution of stored chain length along the tube. This effect could be important for anisotropically deformed network, where the stored length from the compressed (less stretched) sections of the tube will be transferred into more stretched sections. We will discuss this effect in more detail in the future publication.[32]

Our simple estimate of the free energy of the deformed network (17) leads to the stress−strain relation (19), which is practically indistinguishable from the empirical Mooney−Rivlin dependence (20). This provides a microscopic explanation of the nonlinear elasticity of polymer networks. We demonstrated that topological interactions contribute to both phenomenological parameters $2C_1$ and $2C_2$ of the Mooney−Rivlin relation (21).

We would like to stress the qualitative difference between topological entanglements in polymer liquids (solutions and melts) and those in polymer solids (networks and gels). In polymer solutions the topological entanglements reequilibrate and adjust to new thermodynamic conditions (e.g., upon dilution). In contrast to polymer liquids, the topological structure of networks does not change with thermodynamic conditions (e.g., upon deformation) and was fixed once and for all during their preparation. This difference is apparent in the concentration dependence of the tube diameter. The tube diameter of polymer networks changes upon their deformation as $a \sim \lambda^{1/2}$ (eq 22). The deformation factor λ increases with decreasing concentration c as $\lambda \sim c^{-1/3}$ upon network swelling. This leads to a very weak concentration dependence of the tube diameter of swollen networks

$$a_{net} \sim c^{-1/6} \qquad (23)$$

The concentration dependence of tube diameter of polymer solution upon dilution of Θ-solvents[25] $a_{sol} \sim c^{-2/3}$ is much stronger than that in polymer networks (eq 23). The tube diameter of the network at preparation conditions and the diameter of the corresponding solution or melt at the same concentration are of the same order. Upon swelling, the fluctuations in the network are more constrained than those in the solution upon dilution, $a_{net} < a_{sol}$. The topological constraints can be characterized by the number of monomers between entanglements N_e. The topology of the network was frozen in the preparation conditions of high density, and N_e does not change upon swelling. Therefore the tube diameter in a swollen network is smaller than in solutions where the number of monomers between entanglements increases significantly upon dilution $((N_e)_{sol} \sim c^{-4/3}$ in a Θ-solvent[25]).

The main essence of the present paper is in the importance of the nonaffine deformations for the nonlinear elasticity of the entangled networks. These nonaffine deformations are derived from the simplest assumption of the harmonic topological potential (virtual chains) confining Gaussian chains into nonaffinely deformed tubes (eq 22).

Appendix. Fluctuations of Junction Points in a Comb Polymer

Let us calculate the mean square fluctuations $\langle(\Delta R)^2\rangle$ of the junction points connecting the virtual chains to the test one. Such fluctuations can be represented by an effective elastic modulus

$$K_{eff} = kT/\langle(\Delta R)^2\rangle \qquad (A1)$$

of a comb polymer with all of its ends fixed in space. The other ends of side branches (virtual chains of n monomers) of the comb polymer are connected to the backbone. The junction points along the backbone are spaced N monomers apart; see Figure 4a. Note that the
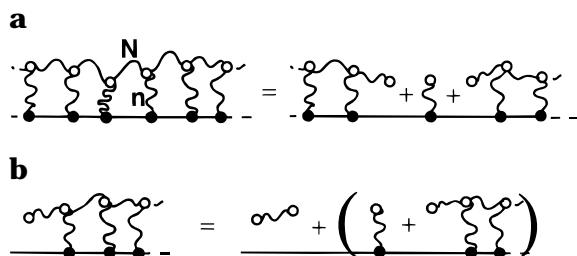
a

b

Figure 4. Elastic modulus of a comb polymer. (a) An infinite comb polymer can be represented as a parallel connection of a virtual chain and two semi-infinite combs. (b) A recurrent scheme can be used for the calculation of the elastic modulus of the semi-infinite comb polymer.

modulus of the comb polymer differs from the modulus $kT/(b^2n)$ of one isolated virtual chain since it is connected in "parallel" to the two semi-infinite comb polymers (see Figure 4a). Indeed, the deformation of one end of this virtual chain leads to the simultaneous deformation of these combs. The effective modulus K_{eff} of such connections of the virtual chain to the two semi-infinite combs with a certain (yet unknown) modulus K is

$$K_{eff} = kT/(b^2n) + 2K \qquad (A2)$$

The value of K can be calculated as the elastic modulus of the sequential connection of two springs: the chain of N monomers and a parallel connection of a virtual chain and one semi-infinite comb (see Figure 4b):

$$\frac{1}{K} = \frac{1}{kT/(b^2N)} + \frac{1}{kT/(b^2n) + K} \qquad (A3)$$

This is a quadratic equation for the modulus K of the semi-infinite comb with the solution

$$K = \frac{kT}{2b^2n}\left[\left(1 + \frac{4n}{N}\right)^{1/2} - 1\right] \qquad (A4)$$

Substituting the modulus of the semi-infinite comb K into eq A2 we get the effective elastic modulus at a junction point

$$K_{eff} = \frac{kT}{b^2n}\left(1 + \frac{4n}{N}\right)^{1/2} \qquad (A5)$$

Comparing eqs A5 and A1, we finally find the following simple result for the mean square fluctuations of the junction point between the test chain and the virtual one

$$\langle(\Delta R)^2\rangle = b^2n\left(1 + \frac{4n}{N}\right)^{-1/2} \qquad (A6)$$

In the limit $N \gg n$ the fluctuations of the junction point are limited by a single virtual chain

$$\langle(\Delta R)^2\rangle \simeq b^2n \quad \text{for} \quad N \gg n \qquad (A7)$$

In this limit the middle sections of the test strands fluctuate much more than the junction points. In the opposite limit, $N \ll n$, the fluctuations of the junction point are controlled by both test chain's segments of N monomers between junction points and by the virtual chains

$$\langle(\Delta R)^2\rangle \simeq b^2(Nn)^{1/2}/2 \quad \text{for} \quad N \ll n \qquad (A8)$$

All the monomers of the test chain have (almost) the same amplitude of fluctuations in this limit.

References and Notes

(1) James, H. M. *J. Chem. Phys.* **1947**, *15*, 651. James, H. M.; Guth, E. *J. Chem. Phys.* **1948**, *11*, 455.
(2) Wall, F. T.; Flory, P. J. *J. Chem. Phys.* **1951**, *19*, 1435. Flory, P. J. *Proc. R. Soc. London* **1976**, A. *351*, 351.
(3) Flory, P. *Principles of Polymer Chemistry;* Cornell University Press: Ithaca, NY, 1971.
(4) Higgs, P. G.; Ball, R. C. *J. Phys. Fr.* **1988**, *49*, 1785.
(5) Bastide, J.; Picot, C.; Candau, S. *J. Macromol. Sci., Phys.* **1981**, *19*, 13. Daoud, M.; Bouchaud, E.; Jannink G. *Macromolecules* **1986**, *19*, 1955.
(6) Edwards, S. F. *Proc. Phys. Soc. (London)* **1967**, *92*, 9.
(7) Higgs, P. G.; Gaylord, R. J. *Polymer* **1990**, *31*, 70.
(8) Treloar, L. R. G. *Rep. Prog. Phys.* **1973**, *36*, 755.
(9) Edwards, S. F.; Vilgis, T. A. *Rep. Prog. Phys.* **1988**, *51*, 243.
(10) Ball, R. C.; Doi, M.; Edwards, S. F.; Wagner, M. *Polymer* **1981**, *22*, 1010.
(11) Marrucci, G. *Rheol. Acta* **1979**, *18*, 484.
(12) Gaylord, R. J. *Polym Bull.* **1983**, *9*, 181.
(13) Ternovskii, F. F.; Khokhlov, A. R. *Sov. Phys. JETP* **1986**, *63*, 728.
(14) Panyukov S. V. *Sov. Phys. JETP* **1988**, *67*, 2274; **1989**, *69*, 342.
(15) For simplicity, we do not consider semidilute solutions with large density fluctuations on scales smaller than the correlation length. The results of this paper can be extended to semidilute solutions using scaling concepts, see: de Gennes, P. G. *Scaling Concepts in Polymer Physics*; Cornell University: Ithaca, NY, 1979.
(16) The correlations in positions of potential cross−links, which appear because of the coherence through the paths connecting these points, can be neglected in our mean field consideration since such correlations give only small fluctuation corrections to the mean field free energy of the dense network.
(17) In the opposite case, $N > n$, the mean square fluctuations of junction points b^2n are smaller than fluctuations of middle sections of the N-mer, b^2N. This leads to a tube with oscillating walls. Since we expect topological entanglements to confine the whole strand rather than individual monomers, this case, $N > n$, is not a good representation of confining potential.
(18) Note that it has to be modified for deformations affecting the volume in swollen networks. The elasticity of virtual springs depends on the polymer concentration in such nonGaussian phantom networks.
(19) If fluctuations of the cross-links are taken into account, the expression for the modulus of a phantom network is modified $G_c = kTc(1 − 2/f)/\bar{N}$, where f is the functionality of cross-links, see section 2.
(20) Ferry, J. D. *Viscoelastic Properties of Polymers*, 3rd ed.; Wiley: New York, 1980.
(21) Bartenev, G. M.; Khazanovich, T. N. *Vysokomol. Soedin.* **1960**, *2*, 20.
(22) Priss, L. S. *Dokl. Akad. Nauk SSSR* **1957**, *116*, 225; *Sov. Phys. Tech. Phys.* **1958**, *3*, 597; *Zh. Tekh. Phys.* **1958**, *28*, 636.
(23) Mooney, M. *J. Appl. Phys.* **1948**, *19*, 434. Rivlin, R. S. *Philos. Trans. R. Soc. London, Ser. A* **1948**, *241*, 379.
(24) Dossin, L. M.; Graessley, W. W. *Macromolecules* **1979**, *12*, 123.
(25) Colby, R. H.; Rubinstein, M. *Macromolecules* **1990**, *23*, 2753.
(26) Pearson, D. S. Doctoral Dissertation, Northwestern University, 1978.
(27) Mark, J. E. *Rubber Chem. Technol.* **1975**, *48*, 494.
(28) Straube, E.; Urban, V.; Pyckhout−Hintzen, W.; Richter, D.; Glinka, C. J. *Phys. Rev. Lett.* **1995**, *74*, 4464. Westermann, S.; Urban, V.; Pyckhout-Hintzen, W.; Richter, D.; Straube, E. *Macromolecules* **1996**, *29*, 6165.
(29) Heinrich, G.; Straube, E. *Acta Polym.* **1983**, *34*, 589; **1984**, *35*, 115.
(30) Heinrich, G.; Straube, E. *Polym. Bull.* **1987**, *17*, 247, 255.
(31) Heinrich, G.; Straube, E.; Helmis, G. *Adv. Polym. Sci.* **1998**, *85*, 33.
(32) Rubinstein, M.; Panyukov, S. To be published.